GEOMETRIC FEATURES BASED FRAMEWORK FOR COLONIC POLYP DETECTION USING A NEW COLOR CODING SCHEME

Dongqing Chen[1]*, Aly A. Farag*[1]*, M. Sabry Hassouna*[2]*, Robert Falk*[3] *and Gerald W. Dryden*[4]

[1] Department of Electrical and Computer Engineering
University of Louisville, Louisville, KY, 40292
[2] Vital Images, Inc., Minnetonka, MN, 55343
[3] Jewish Hospital,Louisville, KY, 40202
[4] Division of Gastroenterology/Hepatology
University of Louisville, Louisville, KY, 40292

ABSTRACT

Curvature-based geometric features have been proven to be important for colonic polyp detection. In this paper, we present an automatic detection framework and color coding scheme to highlight the detected polyps. The key idea is to place the detected polyps at the same locations in a newly created polygonal dataset with the same topology and geometry properties as the triangulated mesh surface of real colon dataset, and assign different colors to the two separated datasets to highlight the polyps. Finally, we validate the proposed framework by computer simulated and real colon datasets. For fifteen synthetic polyps with different shapes and different sizes, the sensitivity is 100%, and false positive is 0. For four real colon datasets, the proposed algorithm has achieved the sensitivity of 75%.

Index Terms— Colorectal cancer, curvature-based geometric features, virtual colonoscopy, color coding

1. INTRODUCTION

Colorectal cancer is the second leading cause of cancer-related death and the third most common form of cancer in the United States [1]. Computer tomographic colonoscopy (CTC), also referred as virtual colonoscopy (VC), is a minimally invasive technique and rapidly evolving diagnostic tool for the location, detection and identification of benign polyps on the early stage before their malignant transformation.

The techniques for colonic polyp detection can be classified into two categories: geometric feature-based approaches, e.g. [2, 3], and statistical feature-based approaches, e.g. [4]. Compared with the statistical methods, geometrical approaches have some advantages: 1) easy and fast implementation, 2) no training data needed, and 3) less computational complexities.

As shown in Figure 1, colonic polyps generally grow from the colonic mucosa, and appear as dome-like structures with small curvedness. The haustral folds appear like shape ridges, which have large curvedness values. The colon walls look nearly flat or cup structure, and they have small curvedness. Several computer aided diagnosis (CAD) schemes based on their geometric features have been proposed [2, 3, 5]. Yoshida and Näppi [2] firstly computed the curvature analysis to characterize polyps, folds and colonic walls in the extracted colon. Finally, they applied fuzzy clustering to the candidates to segment the polyps. Summers *et al*. [3] investigated the feasibility of shape analysis for polyp detection. Huang *et al*. [5] investigated three surface patch fitting methods for curvature estimation. Finally, a shape descriptor sphericity index was defined for colonic polyp detection. All the works mentioned above were dependent on 3D surface curvature estimation, however they suffered from some problems: 1) under discrete cases, $H^2 - K$ in $\kappa_1 = H + \sqrt{H^2 - K}$ and $\kappa_2 = H - \sqrt{H^2 - K}$ for principal curvatures computation can not be always guaranteed to be greater than or equal to zero, where H and K are mean and Gaussian curvature, respectively; 2) κ_1 and κ_2 computed in this way can not provide any direction information; and 3) large neighborhoods for high accuracy increases the computational complexity. The traditional solution to the first problem is that: if $H^2 - K$ is less than 0, κ_1 and κ_2 are simply set to be zeros. In this paper, we estimate the principal curvatures from a 3D triangle mesh surface

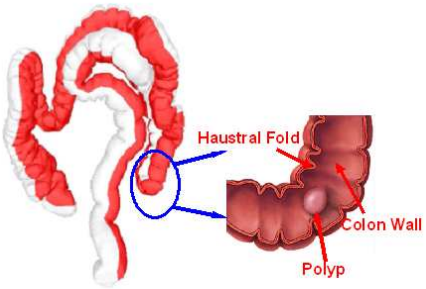

Fig. 1. Three issues include polyp: dome-like structure, folds: ridge-like structure, and colon wall: near flat structure

using the method proposed by Taubin [6]. Then, we propose to use three different geometric features for colonic polyp detection [7]. Finally, we validate the proposed polyp detection framework by computer simulated and real colon datasets and visualize them using a color coding scheme [8]. For 15 synthetic polyps, the sensitivity is 100% with zero false positive. For real colon datasets, the proposed algorithm has achieved the sensitivity of 75%.

2. METHODS

2.1. Principal Curvatures by Fundamental Forms

For a 3D surface, let $p = (x, y, z)$ denote a voxel on the 3D surface **S**, and u and v an orthogonal basis on the plane tangential to **S** at p. If we know the first fundamental forms *E*, *F* and *G*, and second fundamental forms *L*, *M* and *N* of *S*, the Gaussian and mean curvatures K and H are defined as

$$K = \kappa_1\kappa_2 = \frac{LN + M^2}{EG - F^2} \tag{1}$$

$$H = \frac{1}{2}(\kappa_1 + \kappa_2) = \frac{EN - 2FM + GL}{2(EG - F^2)} \tag{2}$$

where, κ_1 and κ_2 are the maximum and the minimum principal curvatures.

If we know the Gaussian curvature and mean curvature, the two principal curvatures can be computed as

$$\kappa_1 = H + \sqrt{H^2 - K} \tag{3}$$

$$\kappa_2 = H - \sqrt{H^2 - K} \tag{4}$$

Unfortunately, there exist some problems in computation of principal curvatures using Gaussian and mean curvatures. The main problems are summarized in Section 1.

We address the problems by using the method proposed in [6]. Please refer Taubin's work [6] for details.

2.2. Geometric Features for Colonic Polyp Detection

Based on accurate curvature estimation, we propose three geometric features for colonic polyp detection: shape index (SI), curvedness (CV) and sphericity ratio (SP).

The SI, CV, and SP at a point p on 3D surface in terms of the principal curvatures are defined as

$$SI = \frac{1}{2} - \frac{1}{\pi} arctan\left(\frac{\kappa_1 + \kappa_2}{\kappa_1 - \kappa_2}\right) \tag{5}$$

$$CV = \sqrt{\left(\frac{\kappa_1^2 + \kappa_2^2}{2}\right)} \tag{6}$$

$$SP = \left|\frac{\kappa_1 - \kappa_2}{H}\right| \tag{7}$$

From the shape index scale as shown in Figure 2 and curvedness, we can easily set thresholds of shape index th_{SI} and curvedness th_{CV} to detect colonic polyps. In this paper, we combine the three above features for colonic polyp detection. The detected results can be computed as $\phi_{detected} = \phi_{SI} \cap \phi_{CV} \cap \phi_{SP}$ where, $\phi_{detected}$, ϕ_{SI}, ϕ_{CV}, ϕ_{SP} denote the numbers of final detection, detected by SI, detected by CV, and detected by SP, respectively.

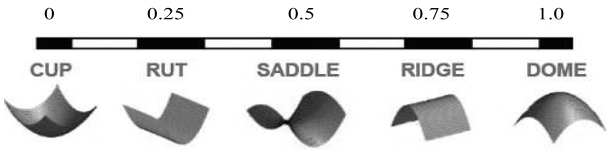

Fig. 2. The shape index scales of 3D geometric shapes

3. AN EASY COLOR CODING SCHEME

In order to facilitate the visual detection of polyps by radiologists while using the VC system, in this section, we propose a new color coding scheme, which is summarized as follows. Compared with other existing color coding methods, our algorithm differs in Step 5 and Step 6. It creates a second polygonal dataset with the exactly same geometry and topology structures with the original 3D CT colon object, then associates polyp and non-polyp candidates with different datasets, finally assigns foreground color to the polyp candidates, and background color to the non-polyp tissues for easy visualization of polyps.

Algorithm (Color Coding Scheme)

1. Reconstructing 3D colon object.
2. Computing curve skeleton of the 3D volumetric colon object and performing fly-through navigation using our methods [9, 10].
3. Creating isosurface of the 3D colon object using the standard *marching cubes* algorithm.
4. Generating the first polygonal dataset of triangle mesh on the isosurface.
5. Creating the second polygonal dataset with exactly same topology and geometry properties with the one in Step 3, but void at each point address.
6. LOOP: During navigation, checking each triangle vertex of the first dataset using Equations 5, 6 and 7.

   1) if it is a polyp candidate, insert the vertex and its neighboring vertices at the same location in the second polygonal dataset.

   2) if not, keep the vertex at the same location in the second polygonal dataset void.

   3) go back to LOOP, until the entire points in the first dataset are finished.

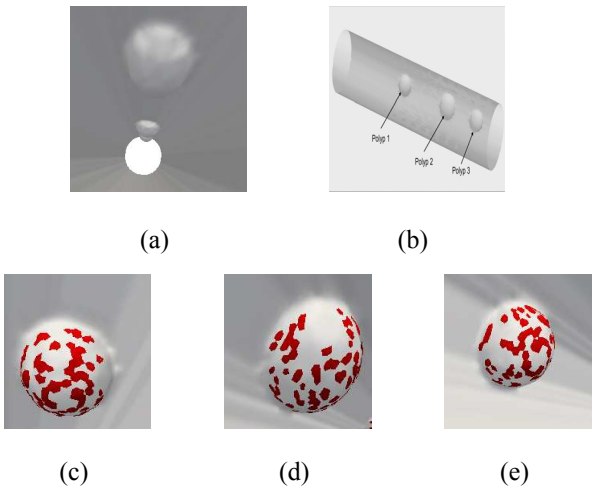

(a) (b)

(c) (d) (e)

Fig. 3. (a) Three sphere-like polyps with different sizes, (b) inserted at different locations, and the detected synthetic polyps as shown in (c), (d) and (e), respectively.

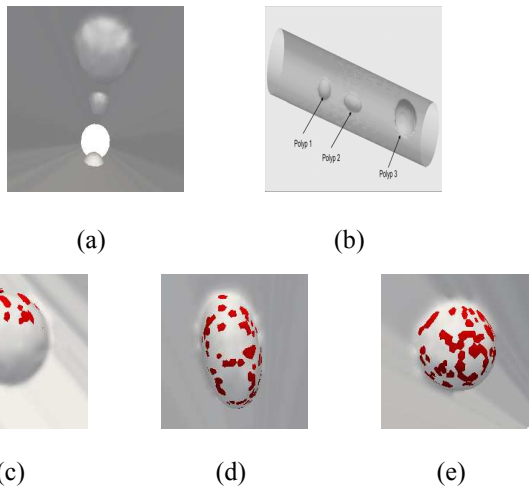

(a) (b)

(c) (d) (e)

Fig. 4. two sphere-like and one ellipse-like polyps, and (d) inserted at different locations as shown on the first row. The second row shows the detected detected synthetic polyps.

7. Assigning background color to the first colon polygonal dataset (containing colon inner wall and haustral folds) and foreground color to the second polygonal dataset (only containing polyp candidates).

4. VALIDATION, RESULTS AND DISCUSSION

In this section, we validate the proposed polyp detection framework using synthetic polyps as well as the real colon datasets.

In experiment I, three sessile sphere-like polyps with different sizes of $8mm$, $10mm$ and $12mm$ are generated as shown in Figure 3(a). And Figure 3(b) shows their locations. The detected polyps are shown in (c), (d) and (e), respectively. In experiment II, two sphere-like polyps with sizes of $10mm$ and $15mm$, and one ellipse-like polyp with size of $12mm$ are generated as shown in Figure 4(a). They are inserted at different locations of the simulated colon as shown in Figure 4(b), and they are placed on the different sides in order to increase the complicity of the simulated phantom. The second row of Figure 4 shows the detected results. Since the phantoms are relatively simple, the false positives are easily removed by the accurately calculated principal curvatures and false positive reduction solution.

In experiment III, five thick spherical folds with diameters ranging from $15mm$ to $60mm$ are simulated in a colonic lumen. Five sessile sphere-like polyps with sizes of $7mm$, $9mm$, $12mm$, $15mm$ and $20mm$, are created and inserted as shown in Figure 5(a). All the polyps as shown in Figure 5(a) are totally detected as shown in Figure 5(b) to Figure 5(f), although the phantom is more complicated than those in Figure 3 and Figure 4(d).

To evaluate the performance of the proposed method, we test our scheme of polyp detection on 4 real colon datasets. We use one clinical colon dataset, which does not contain any real polyps. After the colon lumen is segmented using a seeded region growing algorithm, the colon isosurface is reconstructed. Then, we locate all the boundary points of the 3D colon object, and select four boundary points as the centers, where the five polyps with efficient sizes of $7.5mm$, $9mm$, $15mm$, and $18mm$ are placed from (a) to (d). Among the four polyps, polyp 1 and polyp 2 are inserted on the folds, while the other two are placed in the concave areas between two folds. All the polyps are detected by the proposed detection algorithms and highlighted using red color as shown on the left side in Figure 6.

We have tested it on four clinical colon datasets acquired by Siemens Sensation CT scanner. The dataset volume is $512 \times 512 \times 580$ with voxel size $0.74 \times 0.74 \times 0.75mm^3$. All patients have undergone standard cleansing preparations prior to scan. All the datasets have been examined under optical colonoscopy by an expert radiologist and total 8 polyps with diameter above $5mm$ have been found.

Compared with the high detection rate of synthetic polyps, the algorithm has achieved a sensitivity for the real polyps of 75.0% (6 of 8 polyps) for the four real clinical colon datasets. The results of polyp detection and color coding in the real clinical colon datasets are shown in Figure 7. The two polyps as shown in Figure 7 (c) and (d) are missed by the proposed algorithm, since they have small sizes and irregular shapes.

5. CONCLUSIONS

In this paper, we have proposed an automatic polyp detection framework based on three geometric features and color cod-

(a) phantom (b) polyp 1 (c) polyp 2

(d) polyp 3 (e) polyp 4 (f) polyp 5

Fig. 5. Results of the complicated colon phantom.

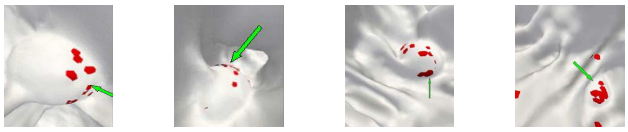

(a) polyp 1 (b) polyp 2 (c) polyp 3 (d) polyp 4

Fig. 6. Detection and color coding results of four synthetic polyps inserted in real colon dataset

ing scheme. The polyp detection framework is validated by the synthetic polyps with different shapes and sizes. For the 15 synthetic polyps, the sensitivity is 100%, and false positive is 0. For four real colon datasets, the proposed algorithm has achieved the sensitivity of 75%. The results show the promise of polyp detection and visualization in this paper.

6. REFERENCES

[1] J. Abbruzzese, "Gastrointestinal cancer," 2004.

[2] H. Yoshida and J. Näppi, "Three-dimensional computer-aided diagnosis scheme for detection of colonic polyps," *IEEE Transactions on Medical Imaging*, vol. 20, no. 12, pp. 1261–1274, 2001.

[3] R.M. Summers, C.F. Beaulieu, L.M. Pusanik, J.D. Malley, R.B. Jeffrey, D.I. Glazer, and S. Napel, "Automated polyp detector for ct colonography: Feasibility study," *Radiology*, vol. 216, no. 12, pp. 284–290, 2000.

[4] Z. Tu, X.S. Zhou, A. Barbu, L. Bogoni, and D. Comaniciu, "Probabilistic 3d polyp detection in ct images: The role of sample alignment," Proceedings of CVPR'06, pp. 1544–1551.

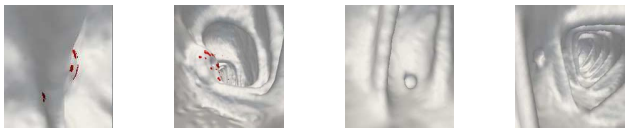

(a) (b) (c) (d)

Fig. 7. Real polyp detection using the proposed detection framework and color coding scheme. (a) and (b) showing two examples of detected polyps, while (c) and (d) showing the two missed polyp with very small sizes and irregular shapes

[5] A. Huang, R.M. Summers, and A.K. Hara, "Surface curvature estimation for automatic colonic polyp detection," in *Proceedings of SPIE 2005*, pp. 393–402.

[6] G. Taubin, "Estiamting the tensor of curvature of a surface from a polyhedral approximation," in *Procceding of ICCV'95*, pp. 902–907.

[7] D. Chen, M.S. Hassouna, A.A. Farag, and R. Falk, "An improved 2d colonic polyp segmentation framework based on gradient vector flow deformable model," Proceedings of MIAR'2006, pp. 372–379.

[8] D. Chen, M.S. Hassouna, A.A. Farag, and R. Falk, "A new color coding scheme for easy polyp visualization in ct-based virtual colonoscopy," Medical Imaging of SPIE 2007, accepted to appear.

[9] M.S. Hassouna and A.A. Farag, "Pde-based three dimensional path planning for virtual endoscopy," in *Proceeding of IPMI'05*, 2005, pp. 529–540.

[10] M.S. Hassouna, A.A. Farag, and R. Falk, "Differential fly-throughs (dft): A general framework for computing flight paths," in *Proceeding of MICCAI'05*, 2005, pp. 654–661.